CHAPTER IV
THE CATALYTIC BEHAVIOR OF NICKEL AND COPPER MONO/BIMETALLIC CATALYSTS IN HYDROGENATION OF METHYL LEVULINATE TO GAMMA-VALEROLACTONE

4.1 Abstract

Recently various supported bimetallic catalysts have been employed as effective catalysts for gamma-valerolactone (GVL) production from levulinic acid or its esters. However, previous reports have shown synergetic roles of active metals and supports as important keys for superior catalytic performance. This work focuses on the role of bimetallic formation between nickel (Ni) and copper (Cu). The experimental results suggest that both Ni and nickel-copper alloy (NiCu) catalysts are good for hydrogenation of methyl levulinate (ML) to an intermediate species, gamma-hydroxypentanoate (HPA). However, only NiCu has a better tendency to accelerate the conversion of HPA to GVL via cyclization process. The NiCu catalyst provided a good performance even at lower temperatures as 140 °C giving 75% of GVL yield within 6 h. In contrast, Ni catalyst showed a comparative performance only at 200 °C, but it exhibited inadequate GVL yield (28%) at 160 °C and gave no catalytic activity below this temperature. Activation energy from experimental study of cyclization step over Ni is about two times larger than that of NiCu (E_a^{K2} values are 121.7 and 56.0 kJ·mol·K^{-1} for Ni and NiCu, respectively) provided strong evidence of superior GVL production over NiCu catalyst.

4.2 Introduction

An increase in energy demand leads to a great challenge for exploring new renewable energy sources. Currently, wind, solar, and thermoelectric sources are considered promising alternatives for sustainable energy. However, with their current energy generation capacities, fossil fuel is still the main energy source. In addition, biomass has been identified as another renewable source of energy that shows high potential for reducing fossil fuel consumption. Lignocellulosic biomass is an abundant material which can be transformed into biofuels and various chemical platforms via biorefinery technology (Alonso et al., 2012; Huber et al., 2006; Kumar et al., 2009; Li et al., 2016) in particular, building block products such as 5-hydroxymethylfurfural (Rosatella et al., 2011), levulinic acid (LA) (Fitzpatrick et al., 2006; Rackemann et al., 2011), and levulinate ester (Amarasekara et al., 2014; Mascal et al., 2010; Peng et al., 2011). These building blocks can be further converted into many value-added products, for example, dimethylfuran, 5-ethoxymethylfurfural, and gamma-valerolactone (GVL) (Climent et al., 2014). Among various products from biomass, GVL has been highly focused in the past few years because of its unique physical and chemical properties as well as its versatile applications (Geboers et al., 2014; Obregon et al., 2014; Putrakumar et al., 2015; Yan et al., 2013). GVL could be used directly as an excellent solvent due to its renewable, non-toxic, and biodegradable characters (Alonso et al., 2013; Fegyverneki et al., 2010; Horvath et al., 2008; Liguori et al., 2015). It has been used as a fuel additive in a similar manner to ethanol. In addition, GVL is considered an interesting precursor to produce bio-based polymers (Chalid et al., 2012; Lee et al., 1998). It is well-known that the production of GVL involves hydrogenation process where LA or its ester could be transformed to GVL in the presence of H_2 gas (Serrano-Ruiz et al., 2010). However, many investigations have shown that the GVL production from LA or its derivatives does not require an external H_2 source. Some catalysts for hydrogenation reactions are also active for catalyzing the decomposition of formic acid (Deng et al., 2009; Hengne et al., 2012). It was proposed that the formic acid decomposed into H_2 and CO_2, H_2 being the reducing agent.

Since the past few years, solid heterogeneous and homogenous metal catalysts have been developed for the reduction of LA, especially noble metals such as

ruthenium (Galletti et al., 2012), platinum (Yan et al., 2009), and palladium (Upare et al., 2011). Among the noble metal catalysts, ruthenium catalysts have shown high performance and selectivity with 97% yield hydrogenation of LA in dioxane as a solvent at 423 K with 5 wt% Ru/C (Manzer, 2004; Upare et al., 2011). For reducing the operation cost, the non-noble metals like copper (Cu) and nickel (Ni) have been tested in this reaction (Shimizu et al., 2014; Upare et al., 2011; Zhang et al., 2015). The high performance of Cu catalyst was achieved by copper chromium combination, where 91% yield of GVL at above 99% conversion of LA (Yan et al., 2013).

Although, LA is the most common building block for GVL production. In 2015, Ding et al. (2015) studied cellulose conversion to methyl levulinate (ML) via alcoholysis. They mentioned that when compared with LA, ML is a non-corrosive biomass derivative with a lower boiling point and viscosity. This makes ML more applicable for its separation from acidic media and more feasible for its use in further reactions. Li et al. (2017) has demonstrated ML production with promising yields from various biomass-derived components including cellulose, starch, sucrose, and monosaccharides using heterogeneous zirconia-zeolite hybrid catalysts. This could pave the way for efficient GVL production from biomass in the future. Yang et al. (2016) prepared GVL from ML using Cu-ZrO_2 as catalysts at various temperatures. They found that the highest GVL selectivity obtained from ML precursor was around 75% at 120 °C after 12 h of reaction time. Another work by Sato et al. (2017) also indicated that the conventional hydrogenation of ML at 250 °C for 5 h gave about 82% of GVL selectivity over Ni/Al_2O_3 catalysts. Cai et al. (2017) studied the catalytic transfer hydrogenation of ethyl levulinate (EL) to GVL with 2-butanol and using 10Cu-5Ni/Al_2O_3 as a catalyst, providing a 97% yield of GVL in 12 h at 150 °C. The common aspect of this work and Cai et al. is that the Ni and Cu catalysts were employed for GVL production from levulinate esters. The good synergy between Ni and Cu provided bimetallic catalysts with high catalytic activity and stability. However, Cai et al. have only studied the metal-supported catalysts and pure support materials, not the performance of the pure nickel or copper catalyst. Therefore, it is worth to expand the promising catalytic transfer hydrogenation (CTH) in such system.

According to the promising CTH reported in previous works for valuable biochemical production from biomass (Li et al., 2016; Yang et al., 2016; Cai et al., 2017), the focus of this work is to study the role of Ni and Cu in terms of catalytic activity and selectivity during CTH process of ML to GVL. The sole nickel-copper alloy (NiCu) catalyst without any supporting materials was prepared, characterized, and tested using 2-propanol as a hydrogen donor.

4.3 Experimental

4.3.1 Chemicals

Chemicals used for Ni metal, Cu metal, and NiCu alloy synthesis included Nickel(II) nitrate hexahydrate ($Ni(NO_3)_2{\cdot}6H_2O$, ≥98%, Ajax Finchem Pty), Copper(II) nitrate trihydrate ($Cu(NO_3)_2{\cdot}3H_2O$, ≥98%, Ajax Finchem Pty). The chemical for catalytic transfer hydrogenation was ML ($CH_3COCH_2CH_2COOCH_3$, ≥98%, Sigma-Aldrich). The chemical used as H-donor for the reaction was Isopropyl alcohol ($(CH_3)_2CHOH$, ≥99.8%, Fisher Scientific UK). The chemical used as solvent for testing with Gas chromatography with flame ionization detector (GC-FID) was ethyl alcohol (CH_3CH_2OH, ≥99.8%, Carlo Erba).

4.3.2 Preparation of Ni metal, Cu metal and NiCu alloy catalysts

Ni metal catalyst was prepared by dissolving 12.21 g $Ni(NO_3)_2{\cdot}6H_2O$ in 10.0 mL of Deionized (DI) water and stirred until a clear solution was obtained. For Cu metal catalyst, 10.15 g of $Cu(NO_3)_2{\cdot}3H_2O$ was dissolved in 10 mL of DI water. For the preparation of NiCu alloy catalyst, a 1:1 molar ratio solution was prepared by dissolving 6.11 g of $Ni(NO_3)_2{\cdot}6H_2O$ and 5.07 g of $Cu(NO_3)_2{\cdot}3H_2O$ in 10 mL of DI water. Each sample was transferred to a crucible and dried at 200 °C with a heating rate of 10 °C·min^{-1} for 2 h, followed by calcination at 800 °C for 5 h at the same heating rate.

After calcination, the catalysts were reduced at 500 °C (heating rate of 3 °C·min^{-1}) for 3 h in a quartz tube reactor within a mixed H_2 and N_2 atmosphere (50:50 %vol) at a total flow rate of 40 mL·min^{-1} prior to the catalytic test.

4.3.3 Catalysts characterization

The crystal structure of catalysts was analyzed by X-ray diffraction (XRD, D8 ADVANCE, Bruker, Ltd., Germany) equipped with monochromatic light source CuK_{α} radiation operating at 40kV and 40 mA, measuring from 2θ = 10 – 80° with step intervals of 0.02° and time intervals of 0.5 s.

The optimal reduction temperature for the catalysts was obtained from temperature-programmed reduction of H_2 (H_2-TPR) analysis (PULSAR, Quantachrome, USA). Each sample was pretreated in a He flow of 30 mL·min^{-1} at 120 °C with the ramping rate of 10 °C·min^{-1} for 60 min and then cooled to 40 °C. The gas feed was then switched to 5% H_2 in Ar with a flow rate of 30 mL·min^{-1} and held at 40 °C for 30 min, before increasing the temperature at a rate of 10 °C·min^{-1} to 850 °C.

The surface morphology of the catalysts was observed by scanning electron microscope (S3400N, Hitachi, Japan) and the catalyst surface compositions were analyzed by energy dispersive spectrometer (SEM-EDS).

The bulk elemental composition of the alloy catalyst was determined by X-ray fluorescence (XRF) (Micro-XRF, Orbis, USA) analysis.

4.3.4 Catalysts testing: Hydrogenation of ML

The reaction was carried out in a 70 mL Teflon lined stainless steel autoclave comprised of 0.58 mL of ML in 24 mL 2-propanol and 1.0 g of catalyst. The reaction mixture was heated up to desired temperature range varying from 120 - 200 °C and held under continuous stirring for a certain period. After cooling, the mixture was filtered 7 and diluted with ethanol with a dilution factor of 10, which was then analyzed by GC-FID (DBWAX column with length 30.0 m × ID 0.25 mm). The initial column temperature was held at 50 °C for 3 min then ramped up to 210 °C at the rate of 40 °C·min^{-1} for 5.5 min. The ML conversion and GVL yields were calculated by Equations (4.1) and (4.2), respectively:

$$\text{ML conversion (\%)} = \left(\frac{\text{mole of initial ML} - \text{mole of final ML}}{\text{mole of initial ML}}\right)100 \quad (4.1)$$

$$\text{GVL yield (\%)} = \left(\frac{\text{mole of obtained GVL}}{\text{mole of initial ML}}\right)100 \quad (4.2)$$

4.4 Results and discussion

4.4.1 Catalysts characterization

Figure 4.1 presents the XRD patterns of the as-prepared catalysts and catalysts. Figure 4.1(a) illustrates the patterns of the as-prepared catalysts. For CuO, the peaks are observed at 2θ values of 32.5, 35.5, 38.7, 48.8, 53.4, 58.3, 61.6, 66.3, 68.0, 72.3, and 74.9°. For NiO, characteristic peaks are evident at 37.14, 43.18, 62.72, 75.38, and 79.3°. The XRD pattern of the NiCuO demonstrates a combination of peaks corresponding to both CuO and NiO. This finding aligns with the research from literature (Wang et al., 2015), which identified NiCuO as a mixed phase of CuO and NiO.

The XRD analysis of Cu, Ni, and NiCu alloy, as shown in Figure 4.1(b), have very similar pattern indicating the FCC structure. The Cu metal showed three diffraction peaks at 43.2, 50.4, and 74.0 °. The Ni metal show diffraction peaks at 44.5, 51.8, and 76.4 °. The NiCu alloy also showed three diffraction peaks at 44.1, 51.3, and 75.5 °. It could be observed clearly that all values of NiCu peaks were in between the peak positions of Cu and Ni, indicating the formation of alloy structure.

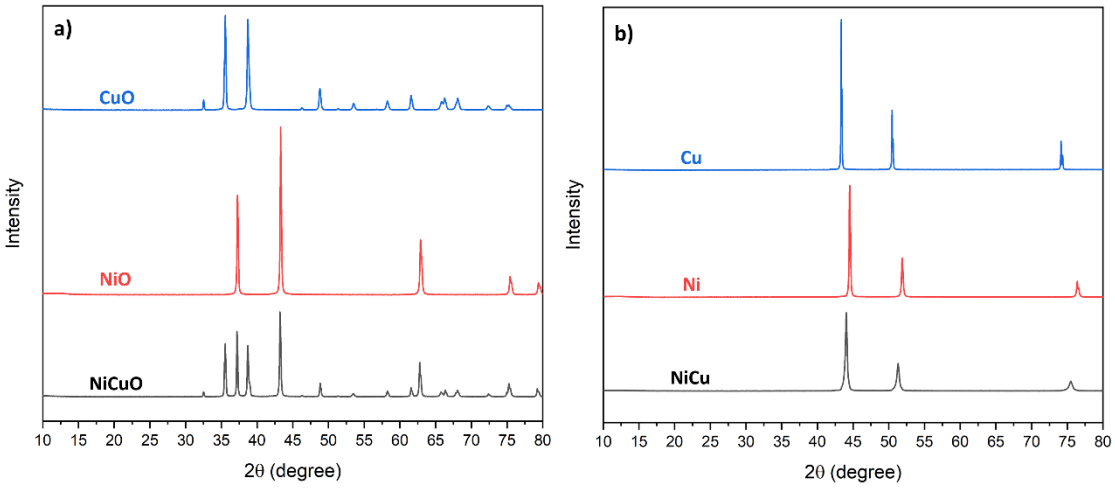

Figure 4.1 XRD of the a) as-prepared catalysts and b) catalysts.

Figure 4.2 shows TPR of the as-prepared catalysts. The reduction of CuO (Figure 4.2(a)) and NiCuO (Figure 4.2(c)) was completed at 400 °C, and NiO (Figure 4.2(b)) at 500 °C, hence the catalyst reduction temperature of 500 °C employed as shown in the methodology section.

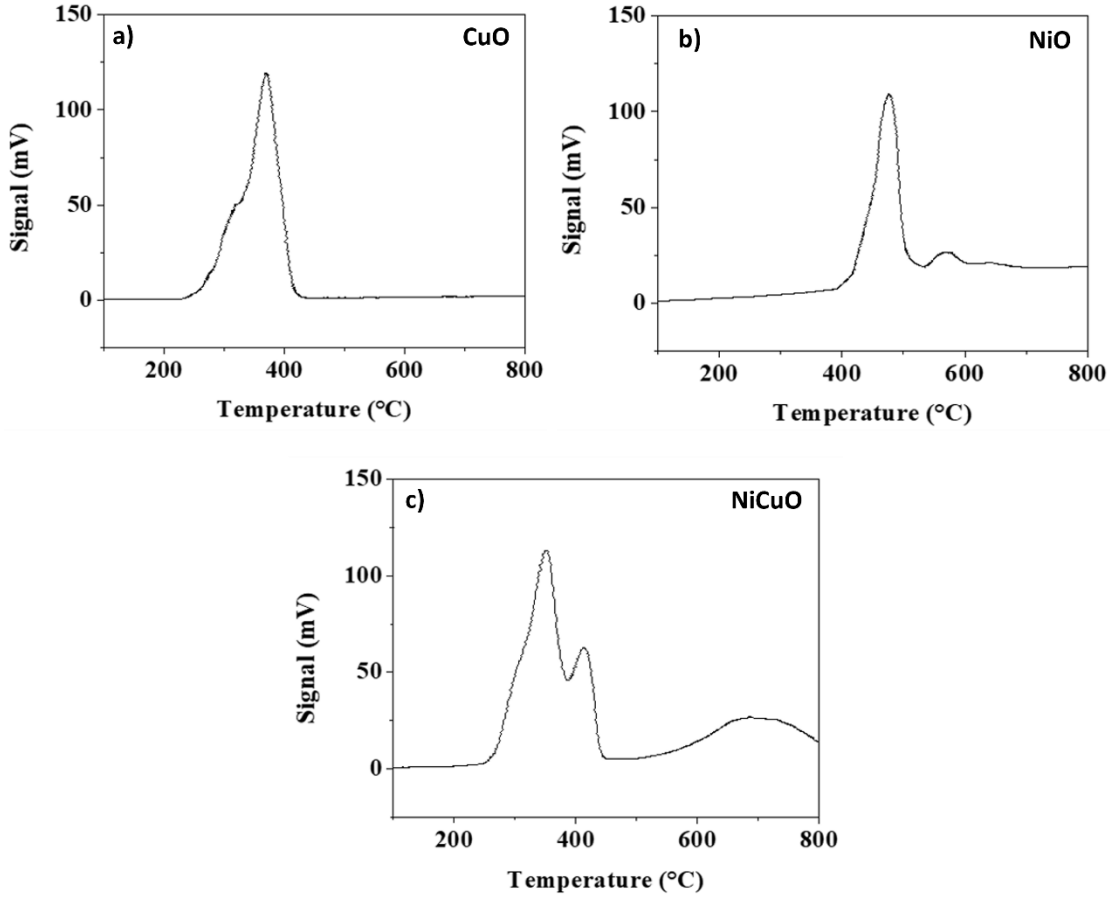

Figure 4.2 H_2-TPR profile of (a) CuO (b) NiO and (c) NiCuO samples.

SEM analysis of the catalysts (Figure 4.3(a-c)) showed that Ni and NiCu were highly dispersed compared to the agglomerated Cu catalyst. Furthermore, the NiCu alloy particles were smaller compared to the Ni metal. EDS element mapping (Table 4.1 and Figure 4.3(d)) of the NiCu alloy showed that Ni tended to disperse on the surface of the catalyst, with 60% of Ni on the surface. XRF result (Table 4.1) revealed that the bulk element of NiCu catalyst is nearly 50% of Ni and Cu, thus confirming that Ni has a slight tendency to accumulate near the surface of the alloy.

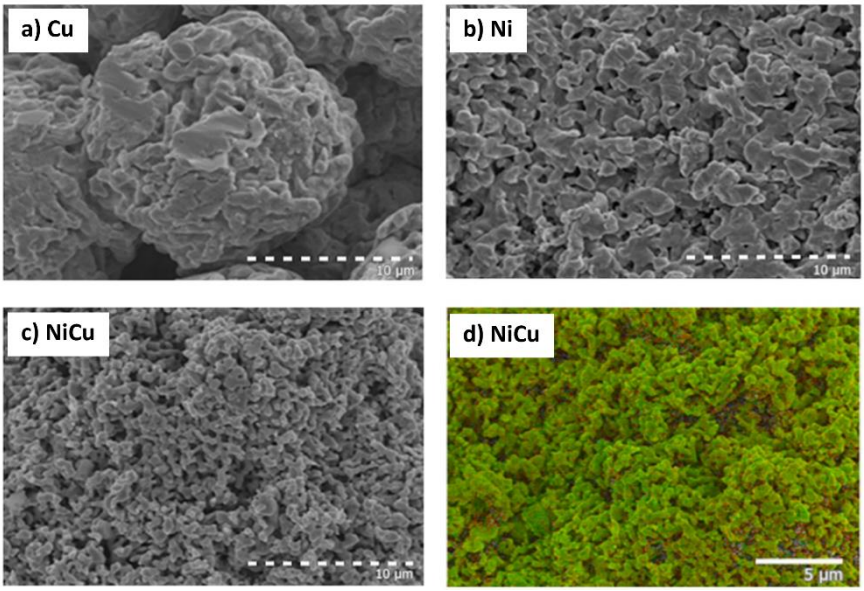

Figure 4.3 SEM images of catalysts (a) Cu metal (b) Ni metal and (c) NiCu alloy catalyst and the EDS element mapping of (d) NiCu alloy (green indicates Ni and Cu is represented by orange).

Table 4.1 Elemental compositions of NiCu catalyst characterized by EDS and XRF.

Catalyst	EDS		XRF	
	Cu (%)	Ni (%)	Cu (%)	Ni (%)
NiCu	40.0	60.0	50.7	49.3

4.4.2 Catalytic behaviors of metal and alloy catalysts

ML conversion to GVL was conducted using Cu, Ni, and NiCu catalysts at 200 °C for 4 h. As displayed in Figure 4.4, Cu had no catalytic performance in ML conversion, similar to the blank test. However, Ni and NiCu showed high catalytic performance indicating promising ML conversion (80% for Ni and 100% for NiCu) and a good GVL yield of 80% for Ni and 100% for NiCu. Although both Ni and NiCu showed their potential for GVL production from ML, the NiCu seemed to exhibit a better conversion and superior GVL selectivity.

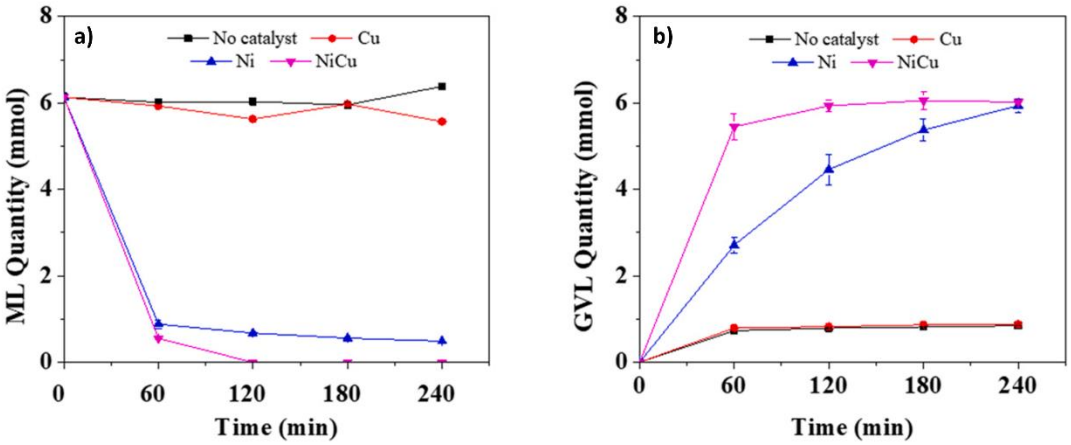

Figure 4.4 Quantity profile of (a) ML and (b) GVL at 200 °C for no catalyst, Cu metal, Ni metal, and NiCu alloy.

Figure 4.5 shows the amount of reactant (ML), intermediate (HPA), product (GVL), and byproduct (methanol, MeOH) during ML hydrogenation when Ni and NiCu catalysts were used with period of 0–180 min. The results clearly showed that the NiCu catalyst system is significantly more effective at producing GVL than the Ni catalyst. The Ni catalyst system exhibits good ML conversion and comparatively high HPA yields for all temperatures, which correlates to the lower GVL yield. Therefore, the Ni catalyst can convert ML to the intermediate but is not selective to the conversion of HPA to GVL. On the other hand, the NiCu catalyst provided roughly twice the GVL yield and half the HPA yield compared to Ni. Despite the good performance in ML conversion of both catalysts, NiCu is able to cyclize the intermediate product, which leads to the GVL formation. Ni is less effective at this process, leading to the high HPA yield, which is exacerbated at lower temperatures.

The reaction pathway is highly selective, with a preference of the formation of GVL. Hence, variation of the temperature from 160 °C to 200 °C when the NiCu catalyst was used had a small effect on the final GVL yield after 3 h (77%, 82%, and 100% at 160 °C, 180 °C and 200 °C, respectively), as shown in Figure 4.5 (a, b, and c, respectively). However, the increase of temperature could improve the reaction rate in terms of ML conversion (0.026, 0.031, 0.051 mmol·min^{-1}, respectively). As shown in Figure 4.5(c), the complete conversion of ML could be achieved within 2 h at 200 °C. Both NiCu (Figure 4.5(c)) and Ni (Figure 4.5(f)) displayed competitive performance at 200 °C, yielding 100%

and 80% GVL respectively. However, Ni catalyst (Figure 4.5(d and e)) showed much poorer performance at the lower temperatures of 160 °C (28% yield), and 180 °C (55% yield).

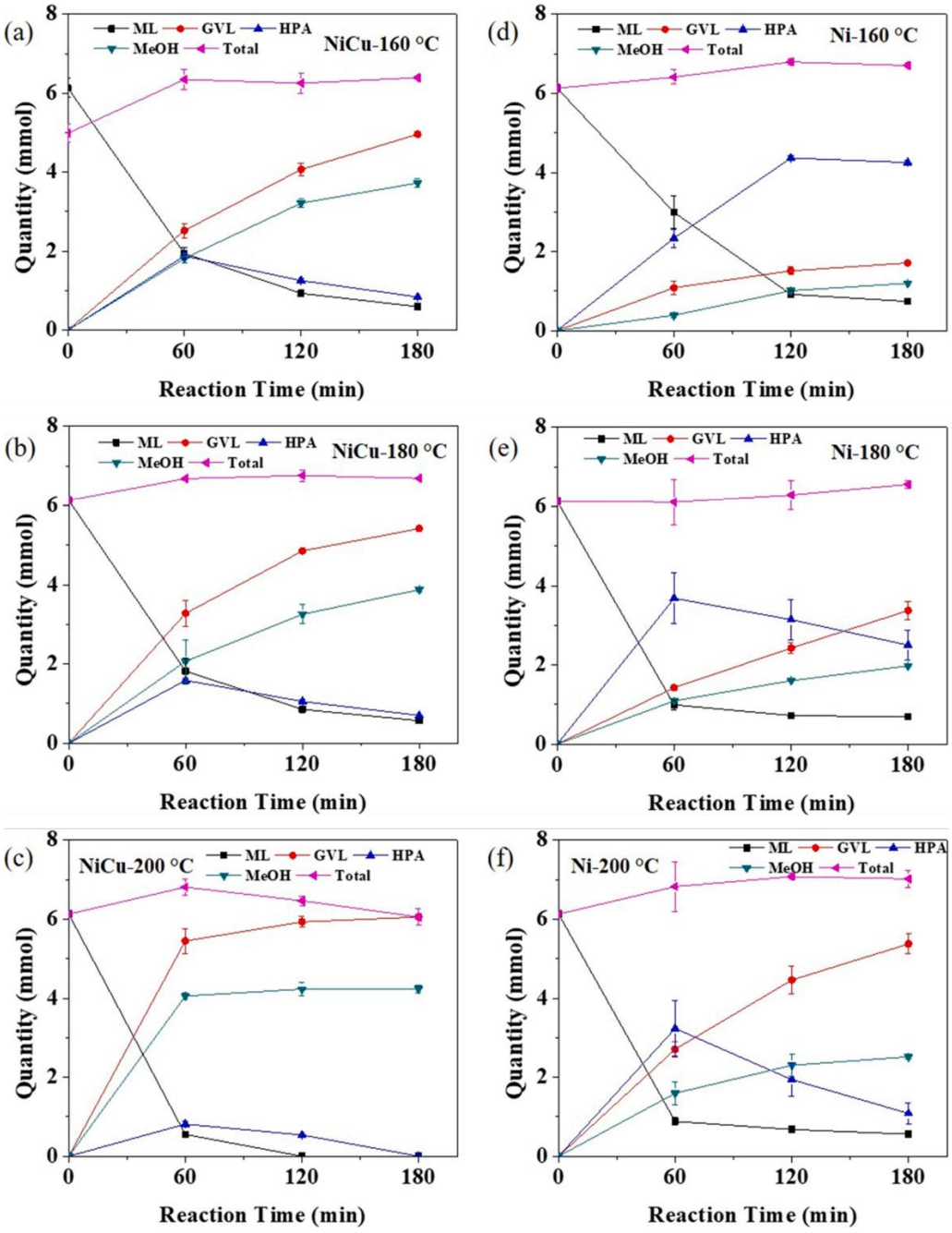

Figure 4.5 Quantity of reactant, product, and intermediate from the hydrogenation of ML in 2-propanol over time using NiCu catalyst at (a) 160 °C (b) 180 °C (c) 200 °C and Ni catalyst at (d) 160 °C (e) 180 °C and (f) 200 °C.

As NiCu catalyst showed superior performance at the lower temperature of 160 °C, it was of interest to study the reaction at even lower temperatures to determine its versatility. Thus, the experiment was conducted at the temperatures of 120 °C and 140 °C and the results are displayed in Figure 4.6. At the temperatures 140 °C and below, NiCu could still produce GVL after an initial period of 2 h. The reaction at 140 °C for 6 h produced a good GVL yield of 75%, whereas at 120 °C, a significantly lower yield of 45% was obtained. Hence, 140 °C is a viable temperature for the production of GVL from the NiCu catalyst system.

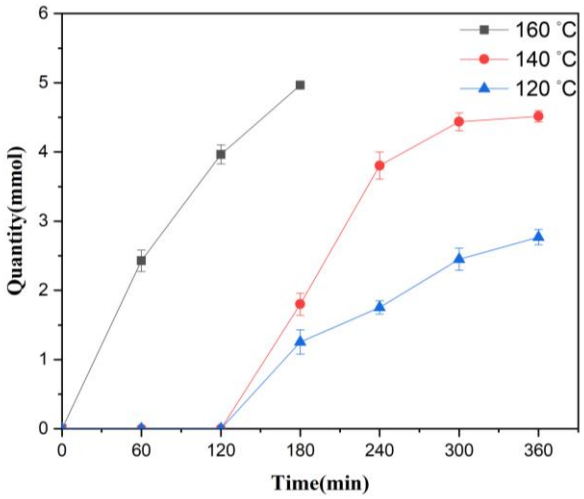

Figure 4.6 A comparison of GVL quantity produced over NiCu catalyst at temperatures of 120–160 °C.

The rate constant (k) and the activation energy (E_a) for the conversion of ML to GVL were calculated from the experimental data (Figure A1 and A2) and displayed in Table 4.2. The conversion of ML to GVL has two key reaction steps as shown in Figure 4.7, with hydrogenation of ML to the intermediate HPA (k_1), followed by the ring-closing process (cyclization) where HPA is converted into GVL (k_2). The rate constants and activation energy were calculated via the Arrhenius equation according to the research performed by (Negahdar et al., 2017). Thus, the rate constants were calculated for each reaction step at 160 °C, 180 °C, and 200 °C, and the activation energies for the catalysts were determined. It was found that the second-order calculations exhibited the best fit for the hydrogenation and cyclization processes.

The hydrogenation activation energy ($\mathbf{E_a^{k1}}$) for both Ni and NiCu catalysts are relatively competitive at 31.5 and 30.7 kJ·mol·K^{-1} respectively. Those values correspond to the similar ML conversion rate as shown in Figure 4.5, with both catalysts exhibiting good performance for ML hydrogenation.

Theoretically, the hydrogenation of ML produces an equivalent quantity of the HPA intermediate, followed by an equal molar concentration of GVL after cyclization. Calculation of E^{k2} a from the obtained k_2 values show significantly higher activation energy for the Ni catalyst (121.7 kJ·mol·K^{-1}) in comparison to that of the NiCu catalyst (56.0 kJ·mol·K^{-1}). This supports the experimental data (Figure 4.5) where Ni catalyst shows higher yields of HPA at 160 ℃ and 180 ℃ in comparison to the NiCu catalyst. At 200 ℃, the high thermal energy enables Ni to produce GVL from HPA cyclization at a comparable rate to NiCu. However, the lower activation energy of NiCu enables the cyclization process to occur even at the lower temperatures of 120 ℃ and 140 ℃ as shown in Figure 4.6, where GVL was not produced when the employed catalyst was Ni.

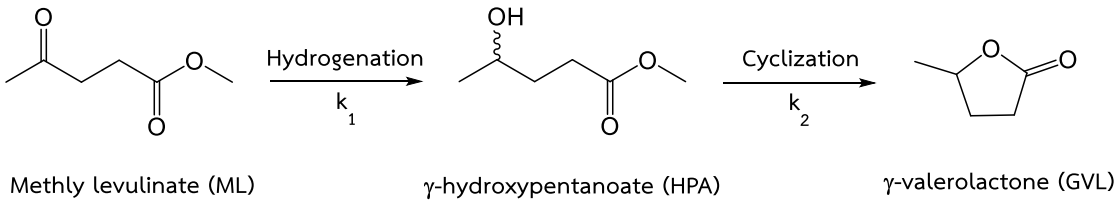

Figure 4.7 Reaction scheme for GVL formation from ML.

Table 4.2 Kinetic calculations for Ni and NiCu catalyst.

Rate constant	Catalyst	k (min^{-1})			E_a (kJ·mol·K^{-1})	R^2
		433 K	453 K	473 K		
k_1	Ni	0.0078	0.0153	0.0162	31.5	0.83
	NiCu	0.0097	0.0121	0.0249	30.7	0.94
k_2	Ni	0.0046	0.0173	0.0806	121.7	0.99
	NiCu	0.00549	0.1014	0.1014	56.0	0.99

4.5 Conclusion

We have shown that GVL could be produced from ML in 2-propanol as a medium via catalytic transfer hydrogenation using NiCu alloy as a catalyst compared with Ni catalysts. At high temperature of 200 °C, either Ni or NiCu achieved high ML conversion and GVL yield. Nevertheless, the NiCu catalyst provided a good performance even at lower temperatures as 140 °C giving 75% of GVL yield within 6 h. In contrast, Ni catalyst showed a comparative performance only at 200 °C, but it exhibited inadequate GVL yield (28%) at 160 °C and gave no catalytic activity below this temperature.

4.6 References

Alonso, D. M., Wettstein, S. G., and Dumesic, J. A. (2012). Bimetallic catalysts for upgrading of biomass to fuels and chemicals. *Chemical Society Reviews, 41*(24), 8075-8098.

Alonso, D. M., Wettstein, S. G., and Dumesic, J. A. (2013). Gamma-valerolactone a sustainable platform molecule derived from lignocellulosic biomass. *Green Chemistry, 15*(3), 584- 595.

Amarasekara, A. S., and Wiredu, B. (2014). Acidic ionic liquid catalyzed one-pot conversion of cellulose to ethyl levulinate and levulinic acid in ethanol-water solvent system. *BioEnergy Research, 7*(4), 1237-1243.

Cai, B., Zhou, X.-C., Miao, Y.-C., Luo, J.-Y., Pan, H., and Huang, Y.-B. (2017). Enhanced catalytic transfer hydrogenation of ethyl levulinate to gamma-valerolactone over a robust Cu–Ni bimetallic catalyst. *ACS Sustainable Chemistry and Engineering, 5*(2), 1322-1331.

Chalid, M., Heeres, H. J., and Broekhuis, A. A. (2012). Green polymer precursors from biomass-based levulinic acid. *Procedia Chemistry, 4*, 260-267.

Climent, M. J., Corma, A., and Iborra, S. (2014). Conversion of biomass platform molecules into fuel additives and liquid hydrocarbon fuels. *Green Chemistry, 16*(2), 516-547.

Deng, L., Li, J., Lai, D.-M., Fu, Y., and Guo, Q.-X. (2009). Catalytic conversion of biomass-derived carbohydrates into gamma-valerolactone without using an external H_2 supply. *Angewandte Chemie International Edition, 48*(35), 6529-6532.

Ding, D., Xi, J., Wang, J., Liu, X., Lu, G., and Wang, Y. (2015). Production of methyl levulinate from cellulose: selectivity and mechanism study. *Green Chemistry, 17*(7), 4037-4044.

Fedorov, A. V., Kukushkin, R. G., Yeletsky, P. M., Bulavchenko, O. A., Chesalov, Y. A., and Yakovlev, V. A. (2020). Temperature-programmed reduction of model CuO, NiO and mixed CuO–NiO catalysts with hydrogen. *Journal of Alloys and Compounds, 844*, 156135.

Fegyverneki, D., Orha, L., Láng, G., and Horváth, I. T. (2010). Gamma-valerolactone based solvents. *Tetrahedron, 66*(5), 1078-1081.

Fitzpatrick, S. W. (2006). The biofine technology: a bio-refinery concept based on thermochemical conversion of cellulosic biomass. *Feedstocks for the Future, 921*, 271-287: American Chemical Society.

Galletti, A. M. R., Antonetti, C., De Luise, V., and Martinelli, M. (2012). A sustainable process for the production of gamma-valerolactone by hydrogenation of biomass-derived levulinic acid. *Green Chemistry, 14*(3), 688-694.

Geboers, J., Wang, X., de Carvalho, A. B., and Rinaldi, R. (2014). Densification of biorefinery schemes by H-transfer with Raney Ni and 2-propanol: A case study of a potential avenue for valorization of alkyl levulinates to alkyl gamma-hydroxypentanoates and gamma-valerolactone. *Journal of Molecular Catalysis A: Chemical, 388-389*, 106-115.

Hengne, A. M., Biradar, N. S., and Rode, C. V. (2012). Surface species of supported ruthenium catalysts in selective hydrogenation of levulinic esters for bio-refinery application. *Catalysis Letters, 142*(6), 779-787.

Horváth, I. T., Mehdi, H., Fábos, V., Boda, L., and Mika, L. T. (2008). Gamma-valerolactone: A sustainable liquid for energy and carbon-based chemicals. *Green Chemistry, 10*(2), 238-242.

Huber, G. W., Iborra, S., and Corma, A. (2006). Synthesis of transportation fuels from biomass: chemistry, catalysts, and engineering. *Chemical Reviews, 106*(9), 4044-4098.

Kumar, P., Barrett, D. M., Delwiche, M. J., and Stroeve, P. (2009). Methods for pretreatment of lignocellulosic biomass for efficient hydrolysis and biofuel production. *Industrial and Engineering Chemistry Research, 48*(8), 3713-3729.

Lee, C. W., Urakawa, R., and Kimura, Y. (1998). Copolymerization of gamma-valerolactone and beta-butyrolactone. *European Polymer Journal, 34*(1), 117-122.

Li, H., Fang, Z., Luo, J., and Yang, S. (2017). Direct conversion of biomass components to the biofuel methyl levulinate catalyzed by acid-base bifunctional zirconia-zeolites. *Applied Catalysis B: Environmental, 200*, 182-191.

Li, H., He, J., Riisager, A., Saravanamurugan, S., Song, B., and Yang, S. (2016). Acid–base bifunctional zirconium n-alkyltriphosphate nanohybrid for hydrogen transfer of biomass-derived carboxides. *ACS Catalysis, 6*(11), 7722-7727.

Liguori, F., Moreno-Marrodan, C., and Barbaro, P. (2015). Environmentally friendly synthesis of gamma-valerolactone by direct catalytic conversion of renewable sources. *ACS Catalysis, 5*(3), 1882-1894.

Manzer, L. E. (2004). Catalytic synthesis of alpha-methylene-gamma-valerolactone: A biomass-derived acrylic monomer. *Applied Catalysis A: General, 272*(1), 249-256.

Mascal, M., and Nikitin, E. B. (2010). High-yield conversion of plant biomass into the key value-added feedstocks 5-(hydroxymethyl)furfural, levulinic acid, and levulinic esters via 5-(chloromethyl)furfural. *Green Chemistry, 12*(3), 370-373.

Negahdar, L., Al-Shaal, M. G., Holzhäuser, F. J., and Palkovits, R. (2017). Kinetic analysis of the catalytic hydrogenation of alkyl levulinates to gamma-valerolactone. *Chemical Engineering Science, 158*, 545-551.

Obregón, I., Corro, E., Izquierdo, U., Requies, J., and Arias, P. L. (2014). Levulinic acid hydrogenolysis on Al_2O_3-based Ni-Cu bimetallic catalysts. *Chinese Journal of Catalysis, 35*(5), 656-662.

Peng, L., Lin, L., Li, H., and Yang, Q. (2011). Conversion of carbohydrates biomass into levulinate esters using heterogeneous catalysts. *Applied Energy, 88*(12), 4590-4596.

Putrakumar, B., Nagaraju, N., Kumar, V. P., and Chary, K. V. R. (2015). Hydrogenation of levulinic acid to gamma-valerolactone over copper catalysts supported on gamma-Al_2O_3. *Catalysis Today, 250*, 209-217.

Rackemann, D. W., and Doherty, W. O. (2011). The conversion of lignocellulosics to levulinic acid. *Biofuels, Bioproducts and Biorefining, 5*(2), 198-214.

Rosatella, A. A., Simeonov, S. P., Frade, R. F. M., and Afonso, C. A. M. (2011). 5-Hydroxymethylfurfural (HMF) as a building block platform: Biological properties, synthesis and synthetic applications. *GreenChemistry, 13*(4), 754-793.

Serrano-Ruiz, J. C., Wang, D., and Dumesic, J. A. (2010). Catalytic upgrading of levulinic acid to 5-nonanone. *Green Chemistry, 12*(4), 574-577.

Shimizu, K.-i., Kanno, S., and Kon, K. (2014). Hydrogenation of levulinic acid to gamma-valerolactone by Ni and MoOx co-loaded carbon catalysts. *Green Chemistry, 16*(8), 3899-3903.

Sun, D., Ohkubo, A., Asami, K., Katori, T., Yamada, Y., and Sato, S. (2017). Vapor-phase hydrogenation of levulinic acid and methyl levulinate to gamma-valerolactone over non-noble metal-based catalysts. *Molecular Catalysis, 437*, 105-113.

Upare, P. P., Lee, J. M., Hwang, Y. K., Hwang, D. W., Lee, J. H., Halligudi, S. B., Hwang, J. S., and Chang, J. S. (2011). Direct hydrocyclization of biomass-derived levulinic acid to 2-methyltetrahydrofuran over nanocomposite copper/silica catalysts. *ChemSusChem, 4*(12), 1749-1752.

Upare, P. P., Lee, J.-M., Hwang, D. W., Halligudi, S. B., Hwang, Y. K., and Chang, J.-S. (2011). Selective hydrogenation of levulinic acid to gamma-valerolactone over carbon-supported noble metal catalysts. *Journal of Industrial and Engineering Chemistry, 17*(2), 287-292.

Wang, Y., Qu, F., Liu, J., Wang, Y., Zhou, J., and Ruan, S. (2015). Enhanced H_2S sensing characteristics of CuO-NiO core-shell microspheres sensors. *Sensors and Actuators B: Chemical, 209*, 515-523.

Yan, K., and Chen, A. (2013). Efficient hydrogenation of biomass-derived furfural and levulinic acid on the facilely synthesized noble-metal-free Cu–Cr catalyst. *Energy, 58*, 357-363.

Yan, K., and Chen, A. (2014). Selective hydrogenation of furfural and levulinic acid to biofuels on the ecofriendly Cu–Fe catalyst. *Fuel, 115*, 101-108.

Yan, K., Jarvis, C., Lafleur, T., Qiao, Y., and Xie, X. (2013). Novel synthesis of Pd nanoparticles for hydrogenation of biomass-derived platform chemicals showing enhanced catalytic performance. *RSC Advances, 3*(48), 25865-25871.

Yan, Z.-p., Lin, L., and Liu, S. (2009). Synthesis of gamma-valerolactone by hydrogenation of biomass-derived levulinic acid over Ru/C catalyst. *Energy and Fuels, 23*(8), 3853-3858.

Yang, Y., Xu, X., Zou, W., Yue, H., Tian, G., and Feng, S. (2016). Transfer hydrogenation of methyl levulinate into gamma-valerolactone, 1,4-pentanediol, and 1-pentanol over Cu–ZrO_2 catalyst under solvothermal conditions. *Catalysis Communications, 76*, 50-53.

Zhang, J., Chen, J., Guo, Y., and Chen, L. (2015). Effective upgrade of levulinic acid into gamma-valerolactone over an inexpensive and magnetic catalyst derived from hydrotalcite precursor. *ACS Sustainable Chemistry and Engineering, 3*(8), 1708-1714.